



## Original article

# Could LogP be a principal determinant of biological activity in 18-crown-6 ethers? Synthesis of biologically active adamantane-substituted diaza-crowns

Fran Supek<sup>a</sup>, Tatjana Šumanovac Ramljak<sup>b</sup>, Marko Marjanović<sup>c</sup>, Maja Buljubašić<sup>d</sup>, Goran Kragol<sup>b</sup>, Nataša Ilić<sup>c</sup>, Tomislav Šmuc<sup>a</sup>, Davor Zahradka<sup>d</sup>, Kata Mlinarić-Majerski<sup>b,\*\*</sup>, Marijeta Kralj<sup>c,\*</sup>

<sup>a</sup> Division of Electronics, Ruder Bošković Institute, Bijenička cesta 54, P.O. Box 180, HR-10002 Zagreb, Croatia

<sup>b</sup> Division of Organic Chemistry and Biochemistry, Ruder Bošković Institute, Bijenička cesta 54, P.O. Box 180, HR-10002 Zagreb, Croatia

<sup>c</sup> Division of Molecular Medicine, Ruder Bošković Institute, Bijenička cesta 54, P.O. Box 180, HR-10002 Zagreb, Croatia

<sup>d</sup> Division of Molecular Biology, Ruder Bošković Institute, Bijenička cesta 54, P.O. Box 180, HR-10002 Zagreb, Croatia

## ARTICLE INFO

## Article history:

Received 5 August 2010

Received in revised form

18 January 2011

Accepted 4 May 2011

Available online 13 May 2011

## Keywords:

Adamantane-substituted diaza-crowns

Biological activity

Crown ethers

Ionophores

Support vector machine

## ABSTRACT

18-crown-6 ethers are known to exert their biological activity by transporting K<sup>+</sup> ions across cell membranes. Using non-linear Support Vector Machines regression, we searched for structural features that influence antiproliferative activity in a diverse set of 19 known oxa-, monoaza- and diaza-18-crown-6 ethers. Here, we show that the logP of the molecule is the most important molecular descriptor, among ~1300 tested descriptors, in determining biological potency ( $R^2_{cv} = 0.704$ ). The optimal logP was at 5.5 (Ghose-Crippen ALOGP estimate) while both higher and lower values were detrimental to biological potency. After controlling for logP, we found that the antiproliferative activity of the molecule was generally not affected by side chain length, molecular symmetry, or presence of side chain amide links. To validate this QSAR model, we synthesized six novel, highly lipophilic diaza-18-crown-6 derivatives with adamantane moieties attached to the side arms. These compounds have near-optimal logP values and consequently exhibit strong growth inhibition in various human cancer cell lines and a bacterial system. The bioactivities of different diaza-18-crown-6 analogs in *Bacillus subtilis* and cancer cells were correlated, suggesting conserved molecular features may be mediating the cytotoxic response. We conclude that relying primarily on the logP is a sensible strategy in preparing future 18-crown-6 analogs with optimized biological activity.

© 2011 Elsevier Masson SAS. All rights reserved.

## 1. Introduction

Since Pedersen in 1967 reported the synthesis of crown ethers, a new class of compounds with unusually powerful cationic non-covalent binding properties [1], they have attracted extensive and continuous attention. Due to their ability in selective binding of metal cations, anions, and neutral molecules, crown ethers have important roles in a variety of applications [1–4]. Many different modifications of the crown ethers, such as changing the ring size, the kind of substituents, and the type of donor atoms, have been synthesized to enhance their complexation properties [5,6].

Because of their structural characteristics, crown ethers exhibit ionophoric properties in membranes, behaving very similarly to the

natural ionophores (such as gramicidin, valinomycin, nonactin, etc.), which makes crown ethers particularly interesting and useful in chemical and biological research and their pharmaceutical potential remains large [4,7]. Naturally occurring ionophores, such as metabolites of microorganisms (e.g. *Streptomyces* sp.) disrupt the flow of ions either into or out of the cell, which dissipates the cellular ion gradients leading to physiological and osmotic stress. Bacteria (particularly Gram-positive bacteria) are very sensitive to this effect [8]. Since cyclic polyethers discriminate among different ions, they can serve as convenient synthetic model compounds for their biological counterparts and they also have similar functions [4]. Indeed, crown ethers were found to be toxic in prokaryotic and eukaryotic cellular systems which led to further studies on their potential for being developed as pharmacological agents [9]. For example, various approaches have been developed to prepare crown-based antimicrobial agents [9–12].

Although the cytotoxic effects of crown ethers on mammalian cells (including tumor cells) were soon recognized, the potential antitumor ability of the compounds has not been scrutinized. The

\* Corresponding author. Tel.: +385 1 4571 235; fax: +385 1 456 1 010.

\*\* Corresponding author. Tel.: +385 1 4680 196; fax: +385 1 4680 195.

E-mail addresses: [majerski@irb.hr](mailto:majerski@irb.hr) (K. Mlinarić-Majerski), [marijeta.kralj@irb.hr](mailto:marijeta.kralj@irb.hr) (M. Kralj).

exceptions are functionalized crown ethers that have been synthetically designed to alkylate and/or cleave DNA in order to achieve antitumor activity [7,13]. In a recent study, we investigated the antiproliferative/antitumor ability of conventional crown ethers of various ring sizes and their derivatives *in vitro* and compared their activity to valinomycin [14]. The results revealed that crown ethers possess marked tumor-cell growth inhibitory activity and that this activity strongly correlates with both the type of hydrophilic cavity (the size and the nature of donor atoms) and the characteristics of hydrophobic ring surrounding, which enhanced the bioactivity by increasing hydrophobicity, possibly due to requirements for membrane insertion. In a different study, a relationship between molecular structure of alkyl-substituted diaza-18-crown-6 derivatives and cytostatic activity in bacteria and yeast was examined [12]. The authors measured that cytotoxic activity in three systems peaks with C<sub>10</sub> and C<sub>12</sub> alkyl side chains, and decreases with either shorter or longer side chains. This discontinuity in toxicity with increasing side chain length was interpreted to result from the interplay of two factors: (i) an increase in hydrophobicity that would be beneficial to activity as it promotes insertion into membranes, and (ii) long chains might interfere with the 'flip-flop' activity (change of orientation in the membrane) that would be essential for K<sup>+</sup> transport and therefore biological activity. Additionally, a presence of a C=O group adjacent to the macroring nitrogen atom in the diaza-crown reduced activity beyond what would be expected by the change in hydrophobicity introduced by the keto group itself.

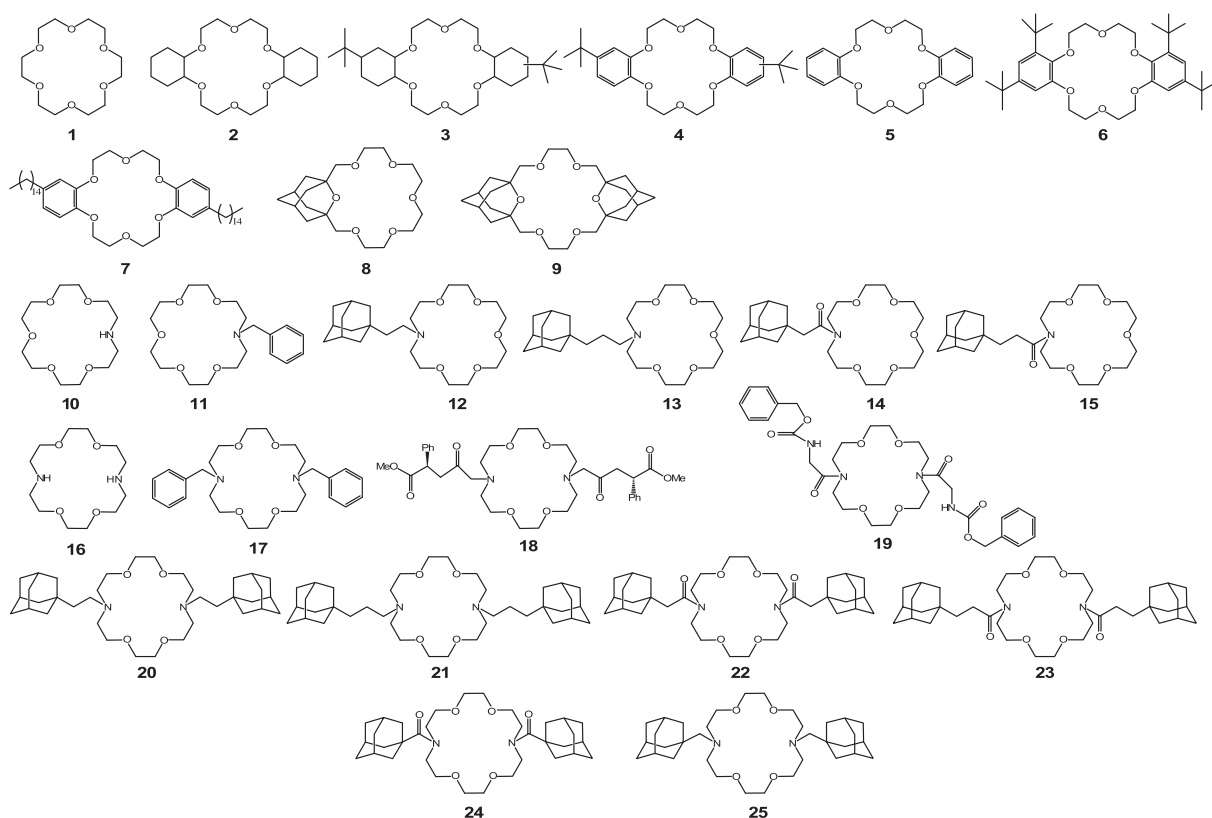
Our motivation for this work was to further investigate the interplay of these molecular features, in particular: hydrophobicity, side chain length, and the side chain amide linkage, on biological activity of 18-crown-6 ethers against cancerous cells and bacteria. The studied compounds include oxa-, monoaza- and diaza-18-

crown-6 and are shown on Scheme 1. Because this set of compounds is diverse with respect to the side substituents, side-chain length and, to some degree, the binding properties of the central ring caused by the type of donor atoms, the rules derived from these compounds should be valid for 18-crown-6 in general. We have measured the cytostatic activity on several human cell lines, as well as on *Escherichia coli* and *Bacillus subtilis* for the series of previously synthesized 18-crown-6 derivatives, oxa-crown ethers **7–9** [15,16], monoaza-crown ethers **10–15** [17], and diaza-crowns ethers **16** and **17**. Furthermore, we have derived a computational structure–activity relationship model that indicated an overarching influence of molecular logP on biological activity, which led us to synthesize six novel lariat diaza-18-crown-6, **20–25**, that contain adamantane moieties in side arms [18]. Finally, we have experimentally verified that the novel compounds are indeed active against cancer cells *in vitro*, as the computational model had predicted.

## 2. Results and discussion

### 2.1. Synthesis

The 2-oxaadmantane containing crown ethers **8** and **9** were prepared from 1,3-bis(hydroxymethyl)-2-oxaadmantane by using an approach based on the literature procedure [15]. The synthetic strategy to prepare monoaza-18-crown-6 **12–15** was based on the coupling reactions of the aza-crown ether **10** with corresponding adamantane derivatives [i.e 1-(2-tosyloxyethyl)adamantane (**26**) [19], 1-(3-tosyloxypropyl)adamantane (**27**) [17] 1-(chloroethanoyl)adamantane (**28**) [20], 1-(chloropropanoyl)adamantane (**29**) [21]. The same strategy was applied for the preparation of adamantane derived diaza-crown ethers **20–23**. The coupling reactions of the



Scheme 1. Structures of crown ethers investigated in this study.

diaza-18-crown-6 (**16**) with corresponding adamantane derivatives **26** and **27** (method a) or the corresponding adamantane acyl chlorides **28** or **29** (method b), followed by reduction of the obtained products with hydride type reagents, in particular  $\text{NaBH}_4$ ,  $\text{B}_2\text{H}_6$ , or  $\text{BH}_3$  THF complex, afforded **20**, **21**, **22**, and **23** (Scheme 2) in 54, 59, 56, and 64% yield, respectively. However, the crown ether **24** was prepared applying the method b from diaza-18-crown-6 (**16**) and 1-adamantanecarbonyl chloride (**30**) in the yield of 65%. The subsequent reduction of **24** using  $\text{LiAlH}_4$  afforded **25** in the yield of 49%.

## 2.2. Biological activity within a diverse set of 18-crown-6 compounds varies depending on the molecular structure

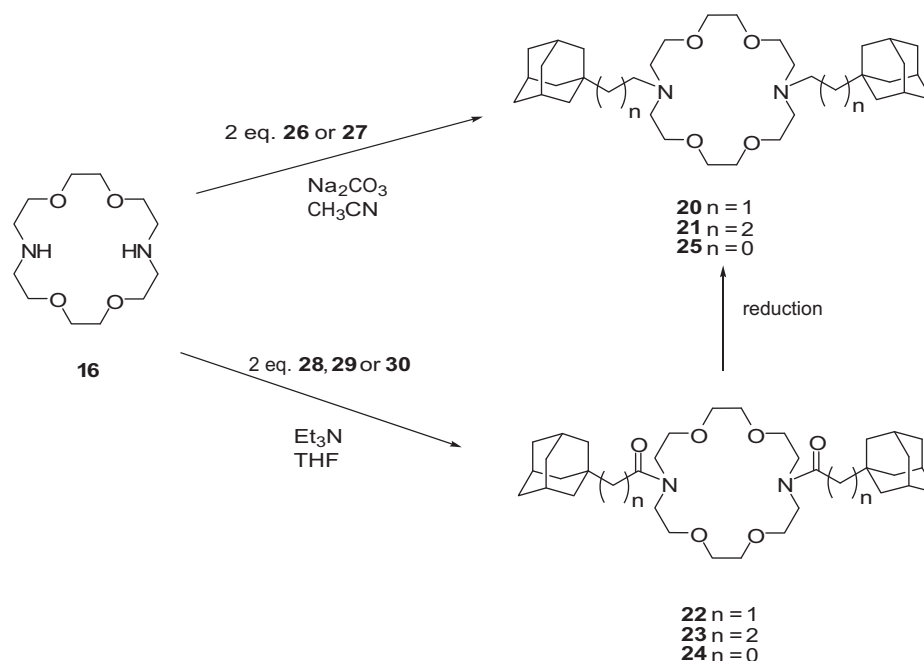
Crown ethers **7–16** and **20–25** were screened for their potential antiproliferative effects on a panel of seven human cell lines, which were derived from different cancer types including H 460 (lung carcinoma), SW 620 (colon carcinoma), MCF-7 (breast carcinoma), MiaPaCa-2 (pancreatic carcinoma), HeLa (cervical carcinoma), HCT-116 (colon carcinoma), and MOLT-4 (lymphoblastic leukemia) (Table 1). As can be seen from the Table 1, the studied compounds differ in the degree of antiproliferative activity on tumor cell lines. Here we discuss the observed differences in light of past investigations of the underlying mechanisms of crown ether biological activity, and the structural features of the molecules which were previously observed to relate to said activity.

Oxa-adamantane crown ethers **8** and **9** were chosen because the incorporation of a rigid polycyclic moiety into crown ethers should affect their conformational mobility and complexation abilities, while the lipophilic moiety (adamantane) should increase the solubility of the crown ethers in nonpolar media (membrane) and thereby increase their ability for ion transport via their complexation with metal ions [15]. As demonstrated, only bis(2-oxaadamantano)-18-crown-6 (**9**) showed significant antiproliferative activity. Bis(4-hexadecyl benzo)-18-crown-6 (**7**) showed very modest antiproliferative activity, presumably because the presence of long alkyl side-chains attached to benzene ring makes this molecule highly lipophilic and thus very slightly soluble in aqueous medium.

Unsubstituted mono- and diaza-18-crown-6 (**10** and **16**, respectively) did not show any antiproliferative activity. On the other hand, substituted aza-18-crown-6 **12–15** showed higher activity, although aza-crown ethers **14** and **15** in which the linkage of the adamantane molecule to the aza-18-crown-6 is achieved through an amide bond showed significantly lower activity compared to **12** and **13**, in which the adamantane is attached by a methylene group. As shown previously, this phenomenon could be related to their extraction capabilities [17]. Namely, the aza-crown ethers **14** and **15** (that have adamantane molecule linked through an amide bond) have very low affinity for alkali cations (especially for potassium ion) and poor extraction capabilities, while **12** and **13** displayed significantly higher selectivity toward the extraction of  $\text{K}^+$ . The lipophilicity is necessary for the potassium extraction [17]. Besides, the potassium complexing abilities were shown to be influenced also by the side chain length between adamantane moiety and the macrocyclic ring in similar compounds [17], whereby the compound with two carbon atoms in the linkage has a better affinity toward alkali cations than the one with three C-atoms. However, the antiproliferative activity was very similar between **12** and **13**, pointing to unclear importance of length of methylene-linkage between adamantane moiety and crown ether ring.

## 2.3. Computational structure–activity relationship analysis of 18-crown-6 reveals logP as the main determinant of bioactivity

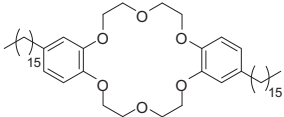
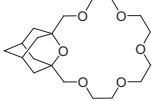

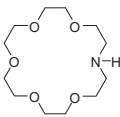
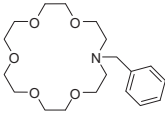
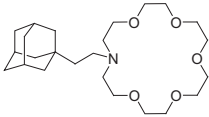
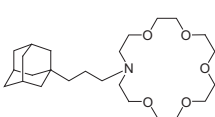
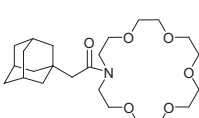
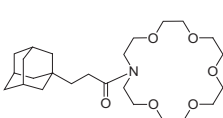
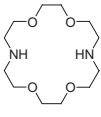
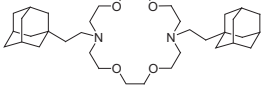
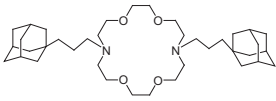
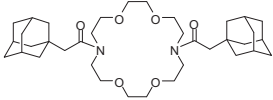
We gathered human tumor cell line cytostatic activity data from our previous investigation of crown ether antitumor activity [14], (Scheme 1, crown ethers **1–6**, **17–19**) and by testing other previously synthesized crown ethers, in particular oxa- and aza-18-crown-6: **7**, **8**, **9**, **12–15** [15–17,22] (Table 1). Using this data, we trained a regression model that would predict antitumor activity from a large number of molecular descriptors (see Experimental Section and Supporting Data). The algorithm employed for this QSAR effort was the Support Vector Machines (SVM) regression. SVMs have desirable properties of robustness to noise and high generalization power in difficult situations with few training



Scheme 2. Syntheses of adamantanyl crown ethers **20–25**.

**Table 1**

In vitro growth inhibition of various tumor cell lines by crown compounds, along with the calculated ALOGP values for each structure 7–25.

Cmpd	Structure	GI <sub>50</sub> <sup>a</sup> (μM)							ALOGP
		H 460	SW 620	MCF-7	MiaPaCa-2	Hela	HCT 116	MOLT-4	
7		63 ± 38	≥100	>100	12 ± 5	25 ± 27	N.T. <sup>b</sup>	N.T.	17.6
8		>100	>100	>100	>100	>100	N.T.	N.T.	0.49
9		4 ± 1	3 ± 1	13 ± 9	2 ± 0	17 ± 3	N.T.	N.T.	1.77
10		>100	>100	>100	N.T.	N.T.	N.T.	N.T.	−1.05
11		>100	>100	>100	N.T.	N.T.	N.T.	N.T.	1.06
12		15 ± 0.6	9 ± 6	8 ± 4	12 ± 0.6	16 ± 0.5	N.T.	N.T.	2.28
13		15 ± 0.1	9 ± 3	6 ± 5	11 ± 2	14 ± 3	N.T.	N.T.	2.74
14		>100	>100	>100	>100	>100	N.T.	N.T.	1.33
15		72 ± 7	13 ± 2	17 ± 5	30 ± 3.4	28 ± 7	N.T.	N.T.	1.79
16		>100	>100	>100	>100	>100	>100	>100	−1.32
20 <sup>c</sup>		4 ± 3	2.6 ± 1.9	4 ± 0.7	1.7 ± 0.6	2.3 ± 1.4	N.T.	N.T.	5.35
21 <sup>c</sup>		1 ± 0.4	1 ± 0.4	2 ± 1	N.T.	N.T.	0.4 ± 0.4	1 ± 1	6.25
22 <sup>c</sup>		14 ± 1	12 ± 5	5 ± 2	N.T.	N.T.	6 ± 0	6 ± 6	3.45

(continued on next page)

Table 1 (continued)

Cmpd	Structure	GI <sub>50</sub> <sup>a</sup> (μM)							ALOGP
		H 460	SW 620	MCF-7	MiaPaCa-2	Hela	HCT 116	MOLT-4	
23 <sup>c</sup>		11 ± 5	19 ± 16	2 ± 0.4	N.T.	N.T.	6 ± 4	3 ± 0.5	4.36
24 <sup>c</sup>		12 ± 0.3	21 ± 7	9 ± 1	N.T.	N.T.	N.T.	N.T.	3.384
25 <sup>c</sup>		18 ± 3	19 ± 2	21 ± 5	N.T.	N.T.	N.T.	N.T.	4.703

<sup>a</sup> GI<sub>50</sub> - the concentration that causes 50% growth inhibition.

<sup>b</sup> N.T. not tested.

<sup>c</sup> Novel compounds synthesized according to computational prediction.

examples and many descriptors, and have consequently become widely popular in other sciences, such as computational biology [23] and proteomics [24]. Examples of previous applications of SVMs in QSAR studies include a classification problem involving dihydrofolate reductase inhibition by pyrimidines [25], large-scale virtual screening of molecular databases for inhibitors of multiple enzymes [26] and prediction of anticancer activity of enkephalin-like peptides containing an unnatural amino acid [27] (for a review, see reference [28]).

The non-linear SVM regression model trained on our 19-compound training set (1–19) using all available molecular descriptors was estimated to predict activity of unknown molecules with some accuracy; the root mean square error (RMSE) was 0.76 log GI<sub>50</sub> units, while squared Pearson's correlation coefficient between measured and predicted values (in crossvalidation) was  $R^2_{cv} = 0.518$ . We were able to considerably improve this result by regressing activity against one molecular descriptor at a time. The highest performing group of descriptors included two computational logP estimates: the Ghose-Crippen ALOGP hydrophobicity [29], with RMSE = 0.63 logs and  $R^2_{cv} = 0.683$  and the Moriguchi MLOGP [30] with RMSE = 0.65 logs and  $R^2_{cv} = 0.645$  (Supporting Data, Table S1). Combining the ALOGP with the MLOGP (squared value) further improved the SVM regression model slightly: RMSE = 0.55 logs,  $R^2_{cv} = 0.753$ , possibly because the combination of two different computational logP estimates may yield a closer approximation of the compounds' true logP values. On the contrary, combining the ALOGP with each of the remaining descriptors did not lead to an appreciable improvement in accuracy of regression over the ALOGP/MLOGP combination (Supporting Data, Table S1), and neither did our attempt to summarize the general trends in molecular descriptors using principal component analysis (Supporting Data, Table S1) as we have done in a previous study [14] of a more structurally diverse set of crown ether molecules.

Thus, in this set of compounds logP is a primary determinant of biological activity, and the relationship of the two variables is non-linear: the predicted activity peaks at about Ghose-Crippen logP = 5.2, and is reduced towards lower or higher logP values (Fig. 1). Molecules with high logP values are poorly soluble in aqueous media thus hindering the activity because the compounds cannot be dissolved in the cell culture medium. Also, the series of alkyl-substituted diaza-18-crown-6 compounds from a previous study by Leevy et al. [12] have been shown to have a similar

relationship of hydrophobicity to activity measured in a different biological system – yeast and bacteria. It is tempting to speculate how the same molecular features may be relevant for toxicity of diaza-18-crown-6 compounds throughout the living world, which is perhaps not unexpected given the similarity of the biological target – the cellular membrane – and given the universal importance of potassium ion homeostasis in cells [31].

#### 2.4. Six novel adamantane-substituted diaza-18-crown-6 are active against cancer cells, in accordance with their logP

The ALOGP-based non-linear regression model (Fig. 1) predicted that the six novel adamantane-containing crown ethers 20–25 (Table 1) would strongly inhibit the growth of cultured cancer cells, and this was indeed shown to be the case. In experimental measurements, the newly synthesized diaza-crown ethers 20–25 showed drastically more pronounced activity than any diaza-crowns previously reported [14]. The crown ethers with

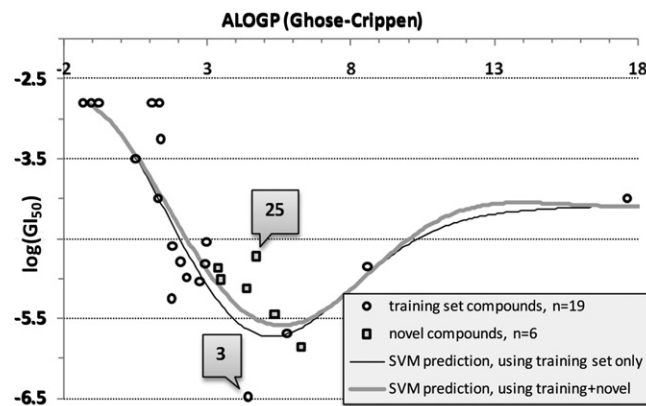
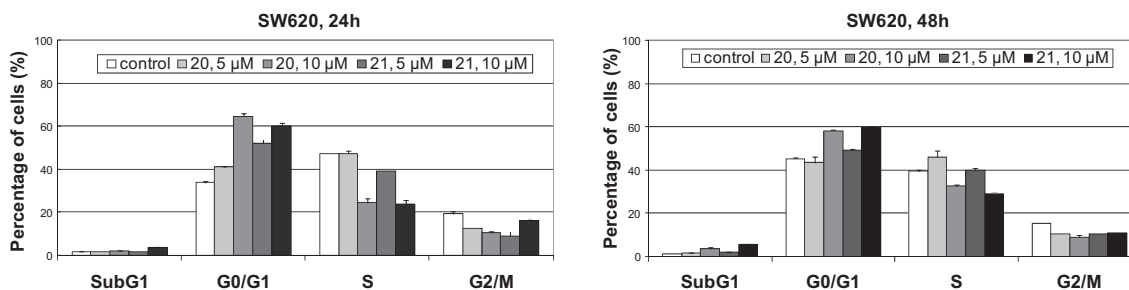


Fig. 1. Biological activity of tested compounds against human cell lines. Points show GI<sub>50</sub> values for a compound - concentration of a compound that inhibits growth of cancer cells by 50%. The curves show a relationship between logP calculated by the Ghose-Crippen ALOGP method [29], and the GI<sub>50</sub> values, as modeled by the non-linear Support Vector Machines regression. The root mean square error of the regression model is 0.58 logs, squared Pearson's correlation coefficient  $R^2 = 0.704$  (both measured in crossvalidation, using all 25 data points). Two compounds that deviate from the model are indicated by callouts.





**Fig. 2.** Cell cycle analysis of SW 620 cells treated with 5 and 10  $\mu$ M compounds **20** and **21**, 24 h, or 48 h. The histograms show percentages of live cells in G0/G1, S or G2/M phase, along with the number of dead (subG1) cells, where subG1 population is expressed as a percentage of total number of measured cells/counts.

adamantane molecule linked through an amide bond **22** and **23** showed a somewhat lower activity than their analogues **20** and **21** having methylene-linked adamantanes, attributable to the additional keto group in **22** and **23** which lowers their logP. However, **24** and **25** exerted very similar activities, meaning that the compound **25** showed a lower activity than the logP-based model predicts. Therefore, it is likely that an additional variable such as e.g. the short side chain length may reduce the activity of **25** (vs. **20** and **21**).

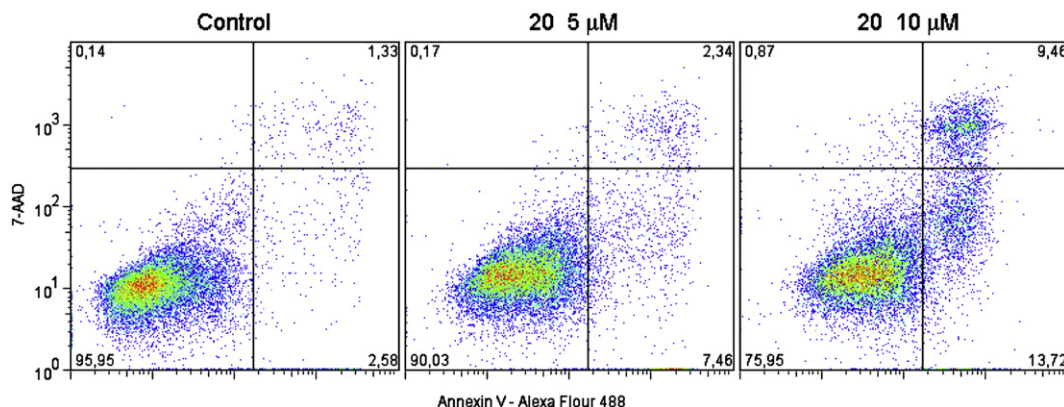
The cell cycle influence-experiments (Fig. 2) showed that the compound having two C-atoms in the linkage (**20**) has a slightly less pronounced effect comparing to **21** (three C-atoms) on the cell cycle of SW 620 cells. Both compounds induced strong G1 phase delay, accompanied with marked S phase reduction, at 5 and 10  $\mu$ M concentration. Also, both compounds induced accumulation of subG1 cells (apoptotic cells) at 10  $\mu$ M concentration. Apoptosis induction was additionally assessed by annexin-V binding assay (Fig. 3). These results are in accordance with our previously published results on the crown ether influence on the cell cycle, which is strong G1 phase delay, along with the activation of apoptosis [14].

To further investigate the relationship of logP to molecular activity and the possible contribution of other structural features of molecules, we combine the initial training set (**1**–**19**) with the six novel compounds **20**–**25** and their experimentally measured activity against cancer cells. The results of SVM regression remained essentially unchanged, with computational logP estimates again having a prominent place among the relevant molecular descriptors (Supporting Information, Table S1). Here, the Ghose-Crippen ALOGP emerges as the most relevant single descriptor (RMS error = 0.58 logs,  $R^2_{cv} = 0.704$ ) and is closely followed by the Moriguchi MLOGP (RMSE = 0.65) and by the dataset with all 1318 descriptors combined (RMSE = 0.65, full data in Supporting Information, Table S1). The optimal value of ALOGP on this expanded set of 25 molecules was found to be 5.5 (Fig. 1). There

is a caveat about how precise is this estimate of the optimal logP: computational logP estimates may not be very accurate, especially with larger molecules – the error of the ALOGP algorithm itself was previously found to range between 0.7 and 1.1 logs [32]. In our 25-molecule dataset, the Ghose-Crippen ALOGP could be complemented by several descriptors that quantify periodicity in distribution of polarizable, voluminous or massive atoms in the molecular structure. Most prominently this included the Moran autocorrelation [33] of lag 4, weighted by atomic polarizability or atomic volume (descriptor names "MATS4p" and "MATS4v"), but also to a similar degree the GETAWAY descriptors [34]: leverage-weighted autocorrelations of lag 5 and 7, weighted by mass ("HATS5m" and "HATS7m"); full data in Supporting Information, Table S1). By including these descriptors alongside the ALOGP, some further reduction of regression error was possible (best RMS error = 0.47, crossvalidation  $R^2_{cv} = 0.803$  for ALOGP + MATS4p). Judging by the magnitude of the error reduction, however, these descriptors are of lesser relevance to biological activity in comparison to the ALOGP.

### 2.5. Symmetry, side chain length, amide side chain linkage, and adamantane moieties: are they relevant for cytostatic activity of 18-crown-6?

Some specific structural features of crown ether molecules were previously discussed as related to biological activity, and we turn to re-examine these effects using our structurally diverse set of 18-crown-6 ethers while controlling for the overarching influence of the compounds' logP. For instance, Gokel and collaborators [12] stated that the increasing length of the alkyl side chains in the examined series of diaza-18-crown-6 compounds is a factor that limits biological activity, and speculated how this might be related to the long side chains interfering with membrane 'flip-flop'



**Fig. 3.** The results of the annexin-V test performed with SW 620 cells after 48 h with crown ether **20**. The results are shown as percentages of viable cells (lower left quadrant), percentages of early apoptotic cells (lower right quadrant) and percentages of late apoptotic cells (upper right quadrant).

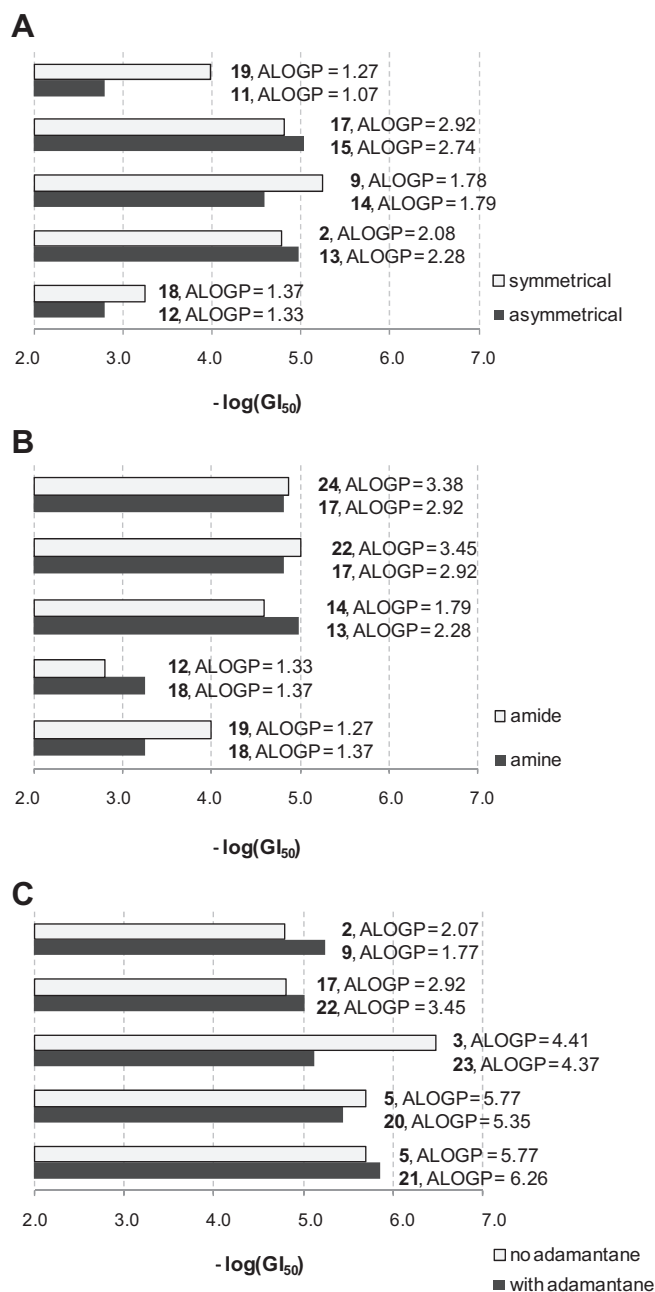
activity necessary for ion transport. In our set of 25 derivatives of 18-crown-6 that contains both diaza-, monoaza- and all-oxa crowns and that also has more diverse substituents, we do not find that the descriptors quantifying substituent length produce highly predictive models either alone or when complemented by Ghose-Crippen ALOGP (Supporting Information, Table S1). The examined descriptors included molecular span ("SPAN",  $R^2_{cv} = 0.410$ ), mass-weighted radius of gyration ("RGyr",  $R^2_{cv} = 0.118$ ), length-to-breadth ratio ("L/Bw",  $R^2_{cv} = 0.408$ ) and asphericity ("ASP",  $R^2_{cv} = 0.292$ ). Let us examine an example from our data: the compounds **5** and **6**, where **6** is much more hydrophobic (ALOGP = 5.7 vs. 8.6), leading to a lower activity predicted by our model as the logP is further from the optimal value of 5.5. In this case the substituent length cannot be applied as an explanation for almost a degree of magnitude difference in biological activity between **5** and **6**. However, the case of compound **25** illustrates a different trend: the logP-based model overestimates its activity (Fig. 1), indicating the very short length of the side chains may have reduced the activity of **25** (compared to **20** or **21**) beyond what would be expected from the logP. Therefore, in addition to the logP, it is possible that the substituent length might be relevant for bioactivity in some specific cases, and it would take a carefully designed experiment to disentangle the two influences.

Our previous work involved finding relevant molecular descriptors that relate to anticancer activity in a set of 15 crown ether-related molecules [14]. The employed set of molecules encompassed crown ethers of varying central ring sizes, their opening derivatives and crown ether fragments. We interpreted the results as the biological activity being dictated by the orientation and asymmetry of hydrophobic groups and the distribution of polarizable elements. Here, we attempt to refine these rather general findings by focusing on a more strictly defined set of molecules: oxa-, monoaza- and diaza-18-crown-6. While the structural features of the central ring ("distribution of polarizable elements", see above) are kept constant, the properties of the substituents and side chains important for membrane insertion can be examined more thoroughly. Here, the logP has emerged as the most relevant molecular feature. In our previous work [14] we had only found a weak (linear) correlation of crown ether logP to biological activity; the difference may be due to the scarcity of the data points in [14], and also to a less structurally consistent set of compounds.

Previously [14] we were not able to clearly determine to what degree the molecular symmetry is relevant to crown ether biological activity, therefore we take the opportunity to investigate this factor in this new set of the 18-crown-6. Five asymmetrical crown ethers **11**, **12**, **13**, **14**, and **15** were matched with symmetrical crown ethers **19**, **18**, **2**, **9**, and **17** respectively, having approximately equal Ghose-Crippen ALOGP values, and their biological activities were compared. We did not find consistently higher activities for the symmetrical molecules (Fig. 4a). Thus, within the examined 18-crown-6 set, molecular symmetry does not appear to play a role in determining cytostatic activity on human cancer cell lines. Next, we have also examined if biological activity is influenced by the type of linkage (amide vs. amine) between the ring of aza-18-crown-6 ether and the side chain, the structural feature discussed previously [12]. Using five ALOGP-matched pairs of compounds, we found no clear regularities of difference in activity of molecules with amine-linked vs. amide-linked side-chains (Fig. 4b). The result obtained by Leevy et al. [12], where the amide group abolished biological activity of diaza-18-crown-6, may be specific to long alkyl side chains ( $C_{10}$  and  $C_{12}$ ) that Leevy et al. [12] used to show this effect. Finally, we employed the same logP-matching approach to test whether the presence of adamantane moiety affects cytostatic activity of crown ethers, and found that adamantane does not add to biological activity of 18-crown-6

beyond what would be expected by its contribution to logP (Fig. 4c).

Our approach of matching crown ethers by their logP would necessarily result in some of the logP-matched pairs of molecules differing in structural features other than the feature currently examined. For instance, we may examine a logP-matched pair to see if symmetry of molecule affects activity, where one of the two molecules may be an oxa-crown ether while the other is a diaza-crown ether. In other words, when examining symmetry, type of bond or presence of particular substituent, the confounding



**Fig. 4.** Comparing cytostatic activity of logP-matched pairs of 18-crown-6 derivatives that differ in a specific structural feature. (A) asymmetrical versus symmetrical molecules, (B) aza- or diaza-18-crown-6 with amine-linked versus amide-linked side chains, (C) compounds containing adamantane versus compounds lacking adamantane. Longer bars denote more active compounds. In all three cases, there was no consistent effect of the examined structural feature of the molecules to biological activity.

variable we control for is the logP, while we do not control other structural features. Even so, the logP-matched compounds are (with a few notable exceptions, see e.g. compound **3** in Fig. 4c) well matched in activity regardless of other possible differences in structure, meaning that the logP does have a prominent role in determining a compound's activity. This rule was derived from a diverse set of 18-crown-6, meaning that (i) it may or may not be applicable for crown ethers of other ring sizes, and that (ii) while it shows a trend valid across various 18-crown-6, this does not rule out that additional structure–activity relationship rules may exist for some specific compounds.

## 2.6. Cytostatic activity of 18-crown-6 derivatives towards bacteria is correlated to activity against human cancer cells

In order to examine whether the same molecular properties are indeed relevant for the biological activity of the 18-crown-6 derivatives in cells of different organisms, we have conducted additional growth inhibition experiments on two common bacteria: *E. coli* and *B. subtilis*. *E. coli* was almost completely resistant to any of the compounds we subjected it to (**2–6, 9, 14, 15, 17, 18** and **20–25**). The highest growth inhibition was recorded for compound **21**, only 26% at the highest tested concentration of  $10^{-4}$  M, corresponding to a  $GI_{50}$  of approx.  $10^{-3}$  M. All other compounds caused *E. coli* growth inhibition  $<15\%$  at  $10^{-4}$  M. *E. coli* is a Gram-negative bacterium, meaning it is enclosed by two layers of membrane; we anticipate that the outer membrane would have to become saturated with the crown ether before the compound enters the inner membrane, and both membranes would need to have some crown ether dissolved in them for the ion transport to take place into the bacterium, or in the other direction. Leevy et al. [12] have also noted that *E. coli* was less susceptible to alkyl-substituted diaza-18-crown-6 compounds than *B. subtilis* or yeast. In our experiments, *B. subtilis* (having a single cell membrane) has indeed proven to be much more sensitive to a structurally more varied set of 18-crown-6 compounds (data in Supporting Table S1). In the sixteen compounds where cytostatic activity to *B. subtilis* was above detection threshold, we found a roughly linear correlation (Fig. 5) between the log  $GI_{50}$  values on human cell lines, and on

*B. subtilis*. A more complex relationship, as captured by a second degree polynomial, fits the data slightly better (Fig. 5, grey line) but the interpretation does not change: the correlation implies that the same molecular features of 18-crown-6 ethers that enable cell killing of human cells are also highly relevant for toxicity to bacterial cells. In designing a hypothetical antimicrobial 18-crown-6 derivative, an insight into the compounds' structural features that cause an increase in the relative bacterial vs. human toxicity would be useful. However, when we regressed the residuals from Fig. 5 against the full set of molecular descriptors using non-linear SVM, we found no relationship (not shown). Thus, the differences in activity against *Bacillus* vs. human cell lines that we did observe are mostly due to measurement noise and not to a genuine difference of biological effect that we could relate to molecular structure. Also note that the linear function in Fig. 5 has a slope  $<1$ , indicating that the toxicity to human cells is predicted to increase faster than the toxicity to bacteria. Taken together with the fact that we found no structural determinants that would relate to increased selectivity against bacteria vs. human cells (see above), one cannot escape the conclusion that 18-crown-6 as a group do not appear promising as antibacterial therapeutics. This is not to say that a few of the 18-crown-6 derivatives are not interesting for future research. In particular, the compound **5** and the novel compound **25** have a favorable ratio of antibacterial vs. human cell cytostatic activity (Fig. 5): they have approx. equal  $GI_{50}$  values in both biological systems (this is actually an encouraging finding; one should keep in mind that bacteria are generally unaffected by antitumor drugs at the concentrations used to treat tumors [35,36]). Regarding the biological mechanism-of-action that leads to bacterial cell death, the 18-crown-6 are analogous to other ionophores which have been recently emerged as medically relevant antimicrobials. For instance, the peptide antibiotic daptomycin that rapidly kills bacteria through  $K^+$  efflux and membrane depolarization [37] has been approved for human use. Daptomycin is effective against Gram-positive bacteria, including difficult-to-treat infectious agents such as methicillin-resistant *Staphylococcus aureus* (MRSA), or vancomycin-resistant enterococci (VRE) [37].

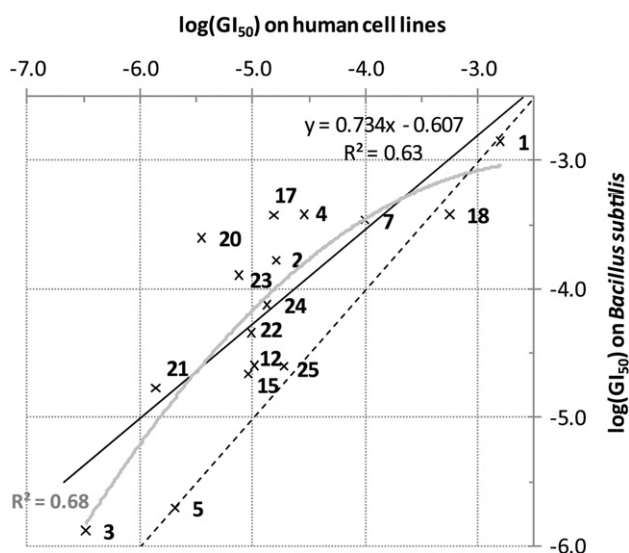
## 3. Conclusions

In summary, we found that the major contribution to biological activity of oxa-, monoaza-, and diaza-18-crown-6 derivatives comes from the logP of the molecule which is determined by hydrophobicity of the attached substituents and side-chains. The optimum logP is approximately at 5.5, while both higher and lower values of the logP are detrimental to activity. Structural features of the tested 18-crown-6 ethers, such as the symmetry of the molecule, type of the substituent, type of the linkage of side chain or side-chain length, did not appear to affect biological activity beyond their contribution to the logP. In addition, we have prepared six new diaza-18-crown-6, **20–25** and experimentally verified the activity predicted by the logP-based model.

## 4. Experimental

### 4.1. Chemistry

IR spectra were recorded on an FT-IR-ABB Bomem MB 102 spectrophotometer in KBr.  $^1H$  and  $^{13}C$  NMR spectra were recorded on a Bruker AV- 300 or 600 MHz. The NMR spectra were taken in  $CDCl_3$  using TMS as a reference and chemical shifts are reported in ppm. HRMS were obtained on an Applied Biosystems 4800 Plus MALDI TOF/TOF instrument (AB, Foster City, CA). Elemental analyses for carbon, hydrogen, and nitrogen were performed on a Perkin–Elmer 2400 elemental analyzer and a Perkin–Elmer series II



**Fig. 5.** Cytostatic activity of 18-crown-6 ethers on the bacterium *Bacillus subtilis* correlates with cytostatic activity on human cancer cell lines. The 16 compounds with activity on *B. subtilis* above detection threshold are shown on the chart (**1–5, 7, 12, 15, 17, 18, 20–25**). The full black line is a linear function fit to the data points; the gray curve is a quadratic curve fit.



CHNS analyzer 2400. The purity of compounds is >95%. Solvents for chromatography were of HPLC purity. All compounds were routinely checked by TLC with Fluka aluminium oxide on TLC-PET foils. 1,3-Bis(hydroxymethyl)-2-oxaadamantane [38], 1-(2-tosyloxymethyl)adamantane (**26**) [19], 1-(3-tosyloxypropyl)adamantane (**27**) [17], 1-(chloroethanoyl)adamantane (**28**) [20], 1-(chloropropanoyl)adamantane (**29**) [21], crown ethers **10** [37], **11** [17], **16** [39,40], **17** [17], were prepared by literature procedure.

#### 4.1.1. General procedure for the preparation of adamantane derived diaza-18-crown-6 ethers **20–25**

**Method a:** In a reaction vessel under a stream of N<sub>2</sub>, two equivalents of corresponding tosylate and one equivalent of diaza-18-crown-6 were dissolved in acetonitrile. To the stirred solution, four equivalents of Na<sub>2</sub>CO<sub>3</sub> were added. The reaction mixture was heated at 80 °C, for five days, after which the reaction mixture was cooled to the ambient temperature and concentrated *in vacuo*. The solid residue was suspended in CH<sub>2</sub>Cl<sub>2</sub>, and filtered through a plug of celite. The combined filtrates were concentrated under reduced pressure to afford oily product. If needed, product was additionally purified by column chromatography.

**Method b:** In a reaction vessel under a stream of N<sub>2</sub>, one equivalent of diaza-18-crown-6 was dissolved in THF, and 2.5 equivalents of triethylamine were added. The resulting mixture was stirred at ambient temperature for 10 min, and a solution of corresponding acyl chloride (two equivalents) was added. The reaction mixture was stirred at ambient temperature for additional 24 h, filtered and the filtrate was evaporated under reduced pressure. The solid residue was suspended in CH<sub>2</sub>Cl<sub>2</sub>, washed with saturated solution of NaCl and dried over anhydrous MgSO<sub>4</sub>. After removal of the solvent, under reduced pressure, the oily product was obtained. The product is additionally purified by column chromatography.

#### 4.1.2. *N,N'*-Bis[2-(1-adamantyl)ethyl]-4,13-diaza-18-crown-6 (**20**)

By following the general procedure (Method a), crown ether **20** was obtained via reaction of 1-(2-tosyloxyethyl)adamantane (**26**, 0.668 g, 0.002 mol) and diaza-18-crown-6 (0.262 g, 0.001 mol). The crude product was purified by column chromatography on Al<sub>2</sub>O<sub>3</sub> (act. II–III) using 0 → 2% MeOH in CH<sub>2</sub>Cl<sub>2</sub> as an eluent, thereby affording 0.317 g (54%) of **20** as a colorless oil. Analytically pure sample was obtained by re-chromatography on a small column of Al<sub>2</sub>O<sub>3</sub> (act. II–III) using 0 → 2% MeOH in CH<sub>2</sub>Cl<sub>2</sub> as an eluent.

<sup>1</sup>H NMR (CDCl<sub>3</sub>) δ/ppm: 1.20–1.30 (m, 4H), 1.47 (br. s, 12H), 1.55–1.75 (m, 12H), 1.92 (br. s, 6H), 2.45–2.60 (m, 4H), 2.70–2.85 (m, 8H), 3.55–3.70 (m, 16H); <sup>13</sup>C NMR (CDCl<sub>3</sub>) δ/ppm: 28.55 (d, 6C), 31.65 (s, 2C), 37.07 (t, 6C), 40.69 (t, 2C), 42.43 (t, 6C), 49.66 (t, 2C), 53.75 (t, 4C), 69.80 (t, 4C), 70.60 (t, 4C); IR (KBr) ν/cm<sup>−1</sup>: 2903 (s), 2852 (s), 1628 (s), 1462 (m), 1133 (m), 1110 (m), 1096 (m); HRMS calculated for [C<sub>36</sub>H<sub>62</sub>N<sub>2</sub>O<sub>4</sub>+H]<sup>+</sup> 587.4782, found 587.4758; Anal. Calcd. for C<sub>36</sub>H<sub>62</sub>N<sub>2</sub>O<sub>4</sub>: C 73.68, H 10.65, N 4.77, found: C 73.12, H 10.23, N 4.46.

#### 4.1.3. *N,N'*-Bis[3-(1-adamantyl)propyl]-4,13-diaza-18-crown-6 (**21**)

By following the general procedure (Method a), crown ether **21** was obtained by reaction of 1-(2-tosyloxypropyl)adamantane (**27**, 1.50 g, 0.0043 mol) and diaza-18-crown-6 (0.563 g, 0.0022 mol). The crude product was purified via column chromatography on Al<sub>2</sub>O<sub>3</sub> (act. II–III) using 0 → 2% MeOH in CH<sub>2</sub>Cl<sub>2</sub> as an eluent, thereby affording 0.783 g (59%) of product as a colorless oil. Analytically pure sample was obtained by re-chromatography on a small column of Al<sub>2</sub>O<sub>3</sub> (act. II–III) using 0 → 2% MeOH in CH<sub>2</sub>Cl<sub>2</sub> as an eluent.

<sup>1</sup>H NMR (CDCl<sub>3</sub>) δ/ppm: 0.95–1.05 (m, 4H), 1.35–1.40 (m, 4H), 1.42 (br. s, 12H), 1.60–1.75 (m, 12H), 1.93 (br. s, 6H), 2.40–2.50 (m, 4H), 2.75–2.80 (m, 8H), 3.50–3.70 (m, 16H); <sup>13</sup>C NMR (CDCl<sub>3</sub>) δ/ppm: 20.09 (t, 2C), 28.66 (d, 6C), 32.06 (s, 2C), 37.16 (t, 6C), 42.12 (t, 2C), 42.43

(t, 6C), 53.81 (t, 4C), 56.92 (t, 2C), 69.91 (t, 2C), 70.65 (t, 6C); IR (KBr) ν/cm<sup>−1</sup>: 2901 (s), 2845 (s), 1645 (s), 1450 (m), 1119 (m); HRMS calculated for [C<sub>38</sub>H<sub>66</sub>N<sub>2</sub>O<sub>4</sub>+H]<sup>+</sup> 615.5095, found 615.5085; Anal. Calcd. for C<sub>38</sub>H<sub>66</sub>N<sub>2</sub>O<sub>4</sub>: C 74.22, H 10.82, N 4.56, found: C 73.99, H 10.44, N 4.26.

#### 4.1.4. *N,N'*-Bis[1-oxo-2-(1-adamantyl)ethyl]-4,13-diaza-18-crown-6 (**22**)

By following the general procedure, (Method b) crown ether **22** was obtained by reaction of diaza-18-crown-6 (0.68g, 0.0026 mol) with 1-(chloroethanoyl)adamantane (**28**, 1.10 g, 0.0052 mol). The crude product was purified via column chromatography on Al<sub>2</sub>O<sub>3</sub> (act. II–III) using 0 → 2% MeOH in CH<sub>2</sub>Cl<sub>2</sub> as an eluent, thereby affording 0.861 g (56%) of product as a colorless oil. Analytically pure sample was obtained by re-chromatography on a small column of Al<sub>2</sub>O<sub>3</sub> (act. II–III) using 0 → 2% MeOH in CH<sub>2</sub>Cl<sub>2</sub> as an eluent.

<sup>1</sup>H NMR (CDCl<sub>3</sub>) δ/ppm: 1.62–1.72 (m, 24 H), 1.97 (br. s, 6H), 2.12 (s, 4H), 3.50–3.70 (m, 24 H); <sup>13</sup>C NMR (CDCl<sub>3</sub>) δ/ppm: 28.38 (d, 6C), 33.37 (s, 2C), 36.54 (t, 6C), 42.42 (t, 6C), 45.48 (t, 1C), 45.56 (t, 1C), 46.33 (t, 1C), 46.57 (t, 1C), 48.97 (t, 1C), 49.18 (t, 1C), 68.97 (t, 1C), 69.63 (t, 1C), 69.81 (t, 1C), 70.08 (t, 1C), 70.22 (t, 1C), 70.39 (t, 1C), 70.44 (t, 1C), 70.59 (t, 1C), 171.17 (s, 1C), 171.24 (s, 1C); IR (KBr) ν/cm<sup>−1</sup>: 2905 (s), 2845 (s), 1449 (m), 1351 (m), 1126 (s); HRMS calculated for [C<sub>36</sub>H<sub>58</sub>N<sub>2</sub>O<sub>6</sub>+H]<sup>+</sup> 615.4368, found 615.4379; Anal. Calcd. for C<sub>36</sub>H<sub>58</sub>N<sub>2</sub>O<sub>6</sub>: C 70.32, H 9.51, N 4.56, found: C 69.99, H 9.26, N 4.64.

#### 4.1.5. *N,N'*-Bis[1-oxo-3-(1-adamantyl)propyl]-4,13-diaza-18-crown-6 (**23**)

By following the general procedure (Method b), crown ether **23** was obtained by reaction of diaza-18-crown-6 (0.63g, 0.0024 mol) with 1-(chloropropanoyl)adamantane (**29**, 1.09 g, 0.0048 mol). The crude product was purified via column chromatography on Al<sub>2</sub>O<sub>3</sub> (act. II–III) using 0 → 2% MeOH in CH<sub>2</sub>Cl<sub>2</sub> as an eluent, thereby affording 1.014 g (64%) of product as a colorless oil. Analytically pure sample was obtained by re-chromatography on a small column of Al<sub>2</sub>O<sub>3</sub> (act. II–III) using 0 → 2% MeOH in CH<sub>2</sub>Cl<sub>2</sub> as an eluent.

<sup>1</sup>H NMR (CDCl<sub>3</sub>) δ/ppm: 1.35–1.45 (m, 4H), 1.47 (br. s, 12H), 1.60–1.75 (m, 12H), 1.95 (br. s, 6H), 2.25–2.35 (m, 4H), 3.55–3.70 (m, 24H); <sup>13</sup>C NMR (CDCl<sub>3</sub>) δ/ppm: 26.18 (t, 1C), 26.30 (t, 1C), 28.29 (d, 6C), 31.65 (s, 2C), 36.80 (t, 6C), 39.19 (t, 1C), 39.22 (t, 1C), 41.88 (t, 6C), 46.45 (t, 1C), 46.77 (t, 1C), 48.44 (t, 1C), 48.62 (t, 1C), 69.09 (t, 1C), 69.67 (t, 1C), 69.78 (t, 1C), 70.07 (t, 2C), 70.20 (t, 1C), 70.41 (t, 1C), 70.59 (t, 1C), 173.86 (s, 1C), 173.91 (s, 1C); IR (KBr) ν/cm<sup>−1</sup>: 2899 (s), 2845 (s), 1450 (m), 1350 (m), 1125 (s), 1071 (m); HRMS calculated for [C<sub>38</sub>H<sub>62</sub>N<sub>2</sub>O<sub>6</sub>+H]<sup>+</sup> 643.4681, found 643.4706; Anal. Calcd. for C<sub>38</sub>H<sub>62</sub>N<sub>2</sub>O<sub>6</sub>: C 70.99, H 9.72, N 4.36, found: C 70.37, H 9.41, N 4.34.

#### 4.1.6. *N,N'*-Bis(1-adamantanoyl)-4,13-diaza-18-crown-6 (**24**)

By following the general procedure (Method b) crown ether **24** was obtained by reaction of diaza-18-crown-6 (0.73 g, 0.0028 mol) with 1-adamantanecarbonyl chloride (**30**, 1.14 g, 0.056). The crude product was purified via column chromatography on Al<sub>2</sub>O<sub>3</sub> (act. II–III) using 0 → 2% MeOH in CH<sub>2</sub>Cl<sub>2</sub> as an eluent, thereby affording 1.074 g (65%) of product as a colorless oil. Analytically pure sample was obtained by re-chromatography on a small column of Al<sub>2</sub>O<sub>3</sub> (act. II–III) using 0 → 2% MeOH in CH<sub>2</sub>Cl<sub>2</sub> as an eluent.

<sup>1</sup>H NMR (CDCl<sub>3</sub>) δ/ppm: 1.72 (br. s, 12H), 1.95–2.05 (m, 18H), 3.50–3.70 (m, 24H); <sup>13</sup>C NMR (CDCl<sub>3</sub>) δ/ppm: 28.39 (d, 6C), 36.47 (t, 6C), 39.08 (t, 6C), 41.95 (s, 2C), 48.53 (t, 4C), 70.14 (t, 4C), 70.62 (t, 4C), 176.87 (s, 2C); IR (KBr) ν/cm<sup>−1</sup>: 2905 (s), 2850 (s), 1615 (s), 1461 (m), 1408 (m), 1228 (m), 1123 (s), 1102 (s), 1067 (s); HRMS calculated for [C<sub>34</sub>H<sub>54</sub>N<sub>2</sub>O<sub>6</sub>+H]<sup>+</sup> 587.4055, found: 587.4060.

#### 4.1.7. *N,N'*-Bis[(1-adamantyl)methyl]-4,13-diaza-18-crown-6 (**25**)

Compound **25** was obtained by reduction of *N,N'*-Bis(1-adamantanoyl)-4,13-diaza-18-crown-6 (**24**) with LiAlH<sub>4</sub>. The solution of

crown ether **24** (0.50 g, 0.00085 mol) in Et<sub>2</sub>O (30 ml) was added dropwise to the suspension of LiAlH<sub>4</sub> (0.213 g, 0.056 mol) in Et<sub>2</sub>O (120 ml). The reaction mixture was heated at the reflux temperature for 7 h. After cooling to the ambient temperature the excess of LiAlH<sub>4</sub> was destroyed by careful dropwise addition of water. The Et<sub>2</sub>O solution was decanted, washed with saturated solution of NaCl and dried over MgSO<sub>4</sub>. After removal of the solvent under reduced pressure the oily product was obtained. The crude product was purified via column chromatography on Al<sub>2</sub>O<sub>3</sub> (act. II–III) using 0 → 2% MeOH in CH<sub>2</sub>Cl<sub>2</sub> as an eluent, thereby affording 0.234 g (49%) of product as a colorless oil. Analytically pure sample was obtained by re-chromatography on a small column of Al<sub>2</sub>O<sub>3</sub> (act. II–III) using 0 → 2% MeOH in CH<sub>2</sub>Cl<sub>2</sub> as an eluent.

<sup>1</sup>H NMR (CDCl<sub>3</sub>) δ/ppm: 1.49 (br. s, 12H), 1.55–1.75 (m, 12H), 1.93 (br. s, 6H), 2.11 (s, 4H), 2.76 (t, 8H, *J* = 6.10 Hz), 3.55–3.65 (m, 16H); <sup>13</sup>C NMR (CDCl<sub>3</sub>) δ/ppm: 28.41 (d, 6C), 34.90 (s, 2C), 37.15 (t, 6C), 41.00 (t, 26C), 56.97 (t, 4C), 70.07 (t, 2C), 70.48 (t, 4C), 70.62 (t, 4C); IR (KBr) ν/cm<sup>−1</sup>: 2899 (s), 2845 (s), 1453 (w), 1292 (w), 1125 (m), 1074 (w); 991 (w); HRMS calculated for [C<sub>34</sub>H<sub>58</sub>N<sub>2</sub>O<sub>4</sub>+H]<sup>+</sup> 559.4469, found: 559.4482.

## 4.2. Biology

### 4.2.1. Antiproliferative activity on tumor cells

The HeLa (cervical carcinoma), MCF-7 (breast carcinoma), SW 620 (colon carcinoma), HCT 116 (colon carcinoma) MiaPaCa-2 (pancreatic carcinoma) and H 460 (lung carcinoma) cells were cultured as monolayers and maintained in Dulbecco's modified Eagle's medium (DMEM), while MOLT-4 cells (acute lymphoblastic leukemia) were cultured in suspension in RPMI medium, both supplemented with 10% fetal bovine serum (FBS), 2 mM L-glutamine, 100 U/mL penicillin and 100 µg/mL streptomycin in a humidified atmosphere with 5% CO<sub>2</sub> at 37 °C.

The growth inhibition activity was assessed as described previously, according to the slightly modified procedure of the National Cancer Institute, Developmental Therapeutics Program [14,41]. Briefly, the cells were inoculated onto standard 96-well microtiter plates on day 0. Test agents were then added in five consecutive 10-fold dilutions (10<sup>−8</sup>–10<sup>−4</sup> mol/L) and incubated for further 72 h. Working dilutions were freshly prepared on the day of testing. The solvent (DMSO) was also tested for eventual inhibitory activity by adjusting its concentration to be the same as in working concentrations (maximal concentration of DMSO was 0.25%). After 72 h of incubation, the cell growth rate was evaluated by performing the MTT assay which detects dehydrogenase activity in viable cells. The absorbency (OD, optical density) was measured on a microplate reader at 570 nm. Each test point was performed in quadruplicate in at least two individual experiments. The results are expressed as GI<sub>50</sub>, which is the concentration necessary for 50% of inhibition. The GI<sub>50</sub> values for each compound are calculated from dose-response curves using linear regression analysis by fitting the test concentrations that give PG (percentage of growth) values above and below the reference value (i.e. 50%). Each result is a mean value from three separate experiments.

### 4.2.2. Cell cycle analysis

The 2 × 10<sup>5</sup> cells were seeded per well, in a 6-well plate. After 24 h, the tested compounds were added at various concentrations. After the desired length of time the attached cells were trypsinized, combined with floating cells, washed with phosphate buffer saline (PBS) and fixed with 70% ethanol. Immediately before the analysis, the cells were washed with PBS and stained with 1 µg/ml of propidium iodide (PI) with the addition of 0.2 µg/µl of RNase A. The stained cells were then analyzed with Becton Dickinson FACScalibur flow cytometer (20000 counts were measured). The percentage of

the cells in each cell cycle phase was determined using ModFit LT™ software (Verity Software House) based on the DNA histograms.

### 4.2.3. Annexin V test

Detection and quantification of apoptotic cells at single cell level, was performed using Annexin V-Alexa 488 conjugate (Molecular Bioprobes, Invitrogen). The cells were seeded in 6-well plates (2 × 10<sup>5</sup> cells/well) and treated according the required schedule. After the desired length of time, both floating and attached cells were collected. The cells were then washed with PBS with the addition of 0.5% BSA, pelleted and resuspended in the Annexin binding buffer (10 mM HEPES, 140 mM NaCl, 2.5 mM CaCl<sub>2</sub>, pH 7.4) containing Annexin V-Alexa 488 conjugate, 7-actinomycin D (7-AAD, Molecular Bioprobes, Invitrogen) according to the manufacturer's recommendations. Camptothecin (10 µM, Sigma) was used as the control apoptosis-inducing agent. The cells were then analyzed on Becton Dickinson FACScalibur flow cytometer (15000 counts were measured). Fluorescence compensation and analysis was performed with FlowJo (TreeStar Inc.). Annexin V positive cells were determined to be early apoptotic and both Annexin V and 7-AAD positive cells were determined to be late apoptotic/necrotic cells. Each test point was performed in duplicate in two individual experiments.

### 4.2.4. Antiproliferative effect on bacteria *B. subtilis* and *E. coli*

Cultures of the bacteria *B. subtilis* and *E. coli* were grown in the Luria-Bertani (LB) medium [42] at 37 °C with shaking, until they reached optical density at 600 nm of approximately 0.1 (OD<sub>600</sub> ≈ 0.1). To determine the colony forming ability before adding the tested compounds, we made series of decimal dilutions in the phosphate buffer (Na<sub>2</sub>HPO<sub>4</sub> × 2H<sub>2</sub>O 0.0333 mol/L, KH<sub>2</sub>PO<sub>4</sub> 0.0333 mol/L), and plated the 10<sup>−6</sup> dilution onto the LB-plates.

At that point (*t* = 0) we divided the starting culture into five aliquots; one of them served as untreated control, whereas in other four we added the tested compounds in the following concentrations: 10<sup>−4</sup> M, 10<sup>−5</sup> M, 10<sup>−6</sup> M and 10<sup>−7</sup> M. Cultures were grown for approximately three mass doubling times (70 min for *B. subtilis* and 105 min for *E. coli*) at 37 °C. Afterwards we made a series of dilutions in the phosphate buffer (described above) and plated the diluted cultures (10<sup>−6</sup> and/or 10<sup>−7</sup> dilutions) onto LB-plates to determine the colony forming ability for the control culture and the percentage of growth inhibition in treated cultures. The plates were incubated overnight at 37 °C and the colonies were counted the next day. The number of colonies formed multiplied by the 1/ dilution yields the number of colony forming units (CFU) per ml. Percent of growth inhibition at a certain concentration of the test compound, and the GI<sub>50</sub> values, were calculated as for the tumor cell assay. Each test point was performed in quadruplicate in at least two individual experiments.

## 4.3. Computational analysis

### 4.3.1. Preparation of data set

Human tumor cell line cytostatic activity data from nine 18-crown-6 derivatives **1–6**, **17–19** was collected from our previous work on anticancer activity of crown ethers in general [14]. Although the GI<sub>50</sub> values were obtained for the five cell lines, only the log GI<sub>50</sub> values obtained for three cell lines (SW 620, MCF-7 and H460) that are represented in previously published measurements (see below) were averaged to obtain an overall estimate of biological activity. The differences in sensitivity of individual cell lines were rather small (see Table 1) and therefore we assumed no relevant information would be lost by the averaging of log GI<sub>50</sub> values over cell lines. Results on antiproliferative activity of compounds **1–6** and **17** were previously published [14] and are additionally provided in Supporting data. We

expanded this set of biological activity with novel bioactivity measurements of other ten crown ethers, here numbered as **7–16**. The overall cytostatic activity was again described as an average  $GI_{50}$  value over the same three human cell lines, grown in identical conditions and measured using the same experimental protocol. These 19 crown ethers with known biological activity constitute our initial training set. In addition to these molecules, the dataset contains six novel diaza-18-crown-6 derivatives **20–25** whose activity was first predicted computationally, then they were synthesized and their biological activity was measured experimentally. The SMILES computational notations of the **25** compounds in our dataset were submitted to the E-Dragon 5.4 web service [43] which predicts a probable three-dimensional structure of the molecules using CORINA [44] and then computes 1666 molecular descriptors per compound. After removal of descriptors invariant within our data, 1318 descriptors remained; to promote re-use by other researchers, this dataset is provided in full in Supporting Information Table S1 and on the authors' website at <http://anticancer.irb.hr/>. We used Marvin 5.1.1 (ChemAxon, <http://www.chemaxon.com>) to visualize, browse, and otherwise handle the molecular structures.

#### 4.3.2. Computational modeling of cytostatic activity from structure

The Support Vector Machines (SVM) algorithm [45] for regression ( $\epsilon$ -SVR variety) was applied to this data, as implemented in the LibSVM software [46] adapted for the Weka 3.5.8 data mining environment [47]. Per recommendation by the LibSVM authors [48], we utilized a radial basis function kernel, and optimized the SVM's meta-parameters "c" and "gamma" in an exhaustive search for a combination yielding the best root-mean-square error (RMSE) estimate on crossvalidation. Gamma was varied exponentially from  $2^{-15}$  to  $2^3$  in steps of  $2^1$ , and c was varied from  $2^{-5}$  to  $2^{15}$  in steps of  $2^1$ . Five runs of four-fold crossvalidation were used to estimate the RMSE, and also the Pearson's correlation coefficient between the predicted and actual values (here denoted as  $R_{cv}$ ). In order to find a single molecular descriptor most informative for prediction of biological activity, the SVM meta-parameter optimization run was repeated for each descriptor separately. The meta-parameters optimal for the whole 1318 descriptor dataset are likely to differ from the meta-parameters optimal for each descriptor, and are also likely to differ between the individual descriptors. The optimal combination of meta-parameters for each descriptor, and the crossvalidation error estimates, are given in Supporting Table S1 and on the authors' website at <http://anticancer.irb.hr/>. In addition to the mean RMSE and  $R_{cv}$  across the five crossvalidation runs, the standard deviation of the RMSE and  $R_{cv}$  were also recorded. A low mean RMSE was the primary criterion for determining if a descriptor is informative, but a lower standard deviation is also desirable since it signifies that the model is robust to the specific choice of molecules in the training set.

#### Acknowledgments

This work was supported by the Croatian Ministry of Science, Education and Sports (Grants no. 098-0982464-2514 to MK; 098-0982933-2911 to KMM; 098-0000000-3168 to TS; 098-0982913-2862 to DZ). The authors are thankful to Dr. Ljerka Tušek Božić for a sample of compound **7**.

#### Appendix. Supplementary material

Supplementary data related to this article can be found online at doi:10.1016/j.ejmech.2011.05.009.

#### References

- [1] C. Pedersen, J. Am. Chem. Soc. 89 (1967) 2495–2496.
- [2] J.S. Bradshaw, R.M. Izatt, A.V. Bordunov, C.Y. Zhu, J.K. Hathaway, in: Comprehensive Supramolecular Chemistry, Pergamon, New York, 1996, p. 35.
- [3] G.W. Gokel, O.F. Schall, in: Comprehensive Supramolecular Chemistry, Pergamon, New York, 1996, p. 97.
- [4] G.W. Gokel, W.M. Leevy, M.E. Weber, Chem. Rev. 104 (2004) 2723–2750.
- [5] R.M. Izatt, K. Pawlak, J.S. Bradshaw, R.L. Bruening, Chem. Rev. 91 (1991) 1721–2085.
- [6] F. Vögtle (Ed.), Host Guest Complex Chemistry, Springer-verlag, Berlin, New York, 1981.
- [7] M. Kralj, L. Tusek-Božić, L. Frkanec, ChemMedChem. 3 (2008) 1478–1492.
- [8] A.J. Houlihan, J.B. Russell, J. Antimicrob. Chemother. 52 (2003) 623–628.
- [9] W. Tso, W. Fung, M.W. Tso, J. Inorg. Biochem. 14 (1981) 237–244.
- [10] W. Tso, W. Fung, Inorg. Chim. Acta 46 (1980) L33–L34.
- [11] W. Tso, W. Fung, Inorg. Chim. Acta 55 (1981) 129–134.
- [12] W.M. Leevy, M.E. Weber, M.R. Gokel, G.B. Hughes-Strange, D.D. Daranciang, R. Ferdani, G.W. Gokel, Org. Biomol. Chem. 3 (2005) 1647–1652.
- [13] S. Vogel, K. Rohr, O. Dahl, J. Wengel, Chem. Commun. (Camb.) (2003) 1006–1007.
- [14] M. Marjanović, M. Kralj, F. Supek, L. Frkanec, I. Piantanida, T. Smuc, L. Tusek-Božić, J. Med. Chem. 50 (2007) 1007–1018.
- [15] K. Mlinarić-Majerski, G. Kragol, Tetrahedron 57 (2001) 449–457.
- [16] K. Mlinarić-Majerski, A. Višnjevac, G. Kragol, B. Kojić-Prodić, J. Mol. Struct. 554 (2000) 279–287.
- [17] K. Mlinarić-Majerski, T. Šumanovac Ramljak, Tetrahedron 58 (2002) 4893–4898.
- [18] M. Kralj, K. Majerski, T. Šumanovac Ramljak, M. Marjanović, Adamantane derivatives of aza-crown ethers and their use in Treatment of tumor (patent application, #P20090355A).
- [19] J.G. Henkel, J.T. Hane, G. Gianutsos, J. Med. Chem. 25 (1982) 51–56.
- [20] W. Lunn, W. Podmore, S. Szinai, J. Chem. Soc. C. (1968) 1657–1660.
- [21] W. Oppolzer, R. Moretti, Tetrahedron 44 (1988) 5541–5552.
- [22] L. Tusek, 1975, Comitato Nazionale Energia Nucleare RT/CHI 1–24.
- [23] A. Ben-Hur, C.S. Ong, S. Sonnenburg, B. Schölkopf, G. Rätsch, PLoS Computational Biol. 4 (2008) e1000173.
- [24] F. Supek, P. Peharec, M. Krsnik-Rasol, T. Smuc, Proteomics 8 (2008) 28–31.
- [25] R. Burbidge, M. Trotter, B. Buxton, S. Holden, Comput. Chem. 26 (2001) 5–14.
- [26] R.N. Jorissen, M.K. Gilson, J. Chem. Inf. Model. 45 (2005) 549–561.
- [27] M. Gredičak, F. Supek, M. Kralj, Z. Majer, M. Hollósi, T. Šmuc, K. Mlinarić-Majerski, S. Horvat, Amino Acids 38 (2010) 1185–1191.
- [28] O. Ivanciuc, in: K. Lipkowitz, T. Cundari, D. Boyd (Eds.), In Reviews in Computational Chemistry, J. Wiley & Sons Inc., Hoboken, NJ, 2007, pp. 291–400.
- [29] A.K. Ghose, G.M. Crippen, J. Comput. Chem. 7 (1986) 565–577.
- [30] I. Moriguchi, S. Hirono, Q. Liu, I. Nakagome, Y. Matsushita, Chem. Pharm. Bull. 40 (1992) 127–130.
- [31] C.D. Bortner, J.A. Cidlowski, Arch. Biochem. Biophys. 462 (2007) 176–188.
- [32] R. Mannhold, G.I. Poda, C. Ostermann, I.V. Tetko, J. Pharm. Sci. 98 (2009) 861–893.
- [33] P.A.P. Moran, Biometrika 37 (1950) 17–23.
- [34] V. Consonni, R. Todeschini, M. Pavan, J. Chem. Inf. Comp. Sci. 42 (2002) 682–692.
- [35] C.A. Bodet, J.H. Jorgensen, D.J. Drutz, J. Antimicrob. Chemother. 28 (1985) 437–439.
- [36] R. Henriksson, S. Holm, B. Littbrand, Acta Oncologica 29 (1990) 43–46.
- [37] J.N. Steenbergen, J. Alder, G.M. Thorne, F.P. Tally, J. Antimicrob. Chemother. 55 (2005) 283–288.
- [38] K. Mlinarić-Majerski, G. Kragol, T. Ramljak, Synlett 2008 (2008) 405–409.
- [39] R.A. Schultz, B.D. White, D.M. Dishong, K.A. Arnold, G.W. Gokel, J. Am. Chem. Soc. 107 (1985) 6659–6668.
- [40] V.J. Gatto, K.A. Arnold, A.M. Viscariello, S.R. Miller, C.R. Morgan, G.W. Gokel, J. Org. Chem. 51 (1986) 5373–5384.
- [41] M. Boyd, K. Paull, Drug Develop. Res. 34 (1995) 91–109.
- [42] J. Sambrook, D.W. Russell, Molecular Cloning: a Laboratory Manual. Cshl Press, 2001.
- [43] I.V. Tetko, J. Gasteiger, R. Todeschini, A. Mauri, D. Livingstone, P. Ertl, V.A. Palyulin, E.V. Radchenko, N.S. Zefirov, A.S. Makarenko, et al., J. Comput. Aided Mol. Des. 19 (2005) 453–463.
- [44] J. Sadowski, J. Gasteiger, G. Klebe, J. Chem. Inf. Comp. Sci. 34 (1994) 1000–1008.
- [45] C.J. Burges, Data Mining Knowledge Discov. 2 (1998) 121–167.
- [46] C.-C. Chang, C.-J. Lin, LIBSVM: A Library for Support Vector Machines Software available at (2001). <http://www.csie.ntu.edu.tw/~cjlin/libsvm>.
- [47] Y. El-Manzalawy, V. Honavar, WLSVM: Integrating LibSVM into Weka Environment Software available at (2005). <http://www.cs.iastate.edu/~yasser/wlsvm>.
- [48] C.-W. Hsu, C.-C. Chang, C.-J. Lin, A Practical Guide to Support Vector Classification. Technical Report, Department of Computer Science, National Taiwan University, 2003. <http://www.csie.ntu.edu.tw/~cjlin>.